

# FOC based control of a surface-mounted permanent magnet synchronous machine (SPMSM)

Barna Temesi

**Abstract**—This short design documentation presents the used system model, parameters and control structure that is used for Field-oriented control (FOC) of a SPMSM. The goal of this control system is to achieve maximum-torque per ampere (MTPA).

*Index Terms*: dynamic modelling of synchronous motors,  $dq$ -reference frame, PMSM

## 1 INTRODUCTION

As in every design process, after the problem statement, the system has to be modeled and analyzed. This starts with an overview of the motor parameters. Next, the motor voltage equations, which are already given in the  $dq$ -reference frame, are examined. The mechanical equation of the motor is also presented.

## 2 MODEL OF THE SYSTEM

The motor in the scope of this design report, is an SPMSM. The load torque is generated using an IM machine which is connected to the SPMSM using a coupling.

Surface mounted PMSM means that the permanent magnets are located on the surface of the rotor. Due to this, the motor is non-salient, and also the reluctance path is equal on the d- and q-axis. This results in equal inductance on the d- and q-axis. For easier understanding, the machine inductance will be denoted as  $L_s$  [2].

$$L_d = L_q = L_s \quad (1)$$

The most important parameters of the motor and the other necessary system parameters are listed in table 1.

As it can be seen from the table, the motor has 4 pole pairs. Generally speaking, this means that the machine is more geared towards high-speed operation. In high-torque operation applications, like in the case of a steering motor, the number of poles might exceed a 100.

In simulations, the total system resistance will be used, which takes into account the resistance of every possible component in the setup [1].

Table 1: System parameters, from previous projects such as

Description	Notation	Value	Unit
Number of pole pairs	$N_{pp}$	4	-
Winding resistance	$R_w$	0.19	$\Omega$
Total system resistance	$R_s$	0.268	$\Omega$
q and d-axis inductance	$L_m$	2.2	mH
Rotor PM flux linkage	$\lambda_{mpm}$	0.12258	wB
Rated speed, SPMSM	$\omega_{m, rated}$	4500	rpm
Rated torque, SPMSM	$\tau_{m, rated}$	20	Nm
Rated power, SPMSM	$P_{m, rated}$	9.4	kW
Rated speed, IM	$\omega_{IM, rated}$	1400	rpm
Rated torque, IM	$\tau_{IM, rated}$	14	Nm
Rated power, IM	$P_{IM, rated}$	2.2	kW
Rated current, VSI	$I_{VSI}$	35	A
IM machine inertia	$J_{IM}$	0.0069	$kg \cdot m^2$
SPMSM machine inertia	$J_{SPMSM}$	0.0048	$kg \cdot m^2$
Total system inertia	$J_{sys}$	0.0146	$kg \cdot m^2$
Coulomb friction	$C$	0.2295	Nm
Viscous friction	$B$	0.0016655	N
Sampling frequency	$f_s$	5000	Hz

The motor voltage equations are shown in equation (2). Due to the assumption that the system is symmetrical and balanced, the zero term ( $v_0$ ) is zero.

$$\begin{aligned} v_d &= R_s i_d + p\lambda_d - \omega_r \lambda_q \\ v_q &= R_s i_q + p\lambda_q + \omega_r \lambda_d \\ v_0 &= 0 \end{aligned} \quad (2)$$

In the  $abc$ -reference frame, the machine flux-linkages are dependent on position. Position-varying inductances are now constant because the model is already transformed into the  $dq0$ -reference frame.

The stator  $dq0$ -reference frame is aligned with the rotor reference frame, which is naturally in the  $dq0$ -reference frame. The rotor  $d$ -axis is chosen to be aligned with the maximum flux density line at no load condition. The  $q$ -axis is always leading the  $d$ -axis by 90 degrees electric. This way, it is aligned with the minimum flux density line [1].

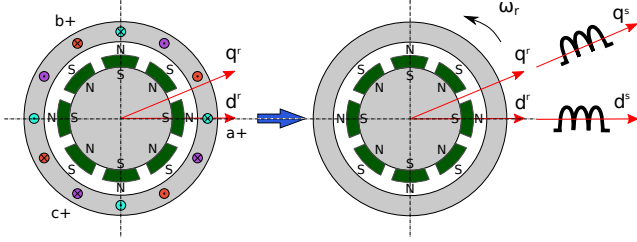


Figure 1: Reference frame transformation from *abc* to *dq*. The structure of the motor is also shown. Inspiration: [3]

The two *d*-axis is in line now. This is convenient because, it results in the *d*-axis and the *q*-axis flux-linkage as shown in equation (3).

$$\begin{aligned}\lambda_d &= (L_{ls} + L_{md}) i_d + \lambda_{mpm} = L_d i_d + \lambda_{mpm} \\ \lambda_q &= (L_{ls} + L_{mq}) = L_q i_q \\ \lambda_0 &= 0\end{aligned}\quad (3)$$

After substitution, the voltage equations may be rewritten as seen in equation (4).

$$\begin{aligned}v_d &= R_s i_d + p(L_d i_d + \lambda_{mpm}) - \omega_r L_q i_q \\ v_q &= R_s i_q + p(L_q i_q) + \omega_r (L_d i_d + \lambda_{mpm})\end{aligned}\quad (4)$$

Where  $p$  is the differential operator  $\frac{d}{dt}$ . Differentiating the equation, keeping in mind that the derivative of a constant is zero, will result in the following.

$$\begin{aligned}v_d &= R_s i_d + L_d \cdot p i_d - \omega_r L_q i_q \\ v_q &= R_s i_q + L_q \cdot p i_q + \omega_r (L_d i_d + \lambda_{mpm})\end{aligned}\quad (5)$$

In one more step, the homogeneous first-order differential equation of the system is acquired.

$$\begin{aligned}\frac{d}{dt} i_d &= -\frac{R_s}{L_d} i_d + \frac{1}{L_d} v_d + \omega_r \frac{L_q}{L_d} i_q \\ \frac{d}{dt} i_q &= -\frac{R_s}{L_q} i_q + \frac{1}{L_q} v_q - \omega_r \frac{L_d}{L_q} i_d - \frac{1}{L_q} \omega_r \lambda_{mpm}\end{aligned}\quad (6)$$

Equations (4) also contain the back-EMF voltage components which are important to highlight here:

$$\begin{aligned}e_d &= -\omega_r L_q i_q \\ e_q &= \omega_r (L_d i_d + \lambda_{mpm})\end{aligned}\quad (7)$$

The governing torque equation can be derived from the equation of the input power of the windings. Simplifying this equation, using the attributions of the SPMSM machine, yields the following expression:

$$T_e = \frac{3}{2} N_{pp} (\lambda_d i_q - \lambda_q i_d) \quad (8)$$

$$T_e = \frac{3}{2} \frac{N_{poles}}{2} (\lambda_{mpm} i_q + (L_d - L_q) i_d i_q) \quad (9)$$

$$T_e = \frac{3}{2} N_{pp} (\lambda_{mpm} i_q) \quad (10)$$

Using Newton's second law, the mechanical equation of the system can be derived as shown in equation (11) [1].

$$T_e = J_{red} \frac{d\omega_m}{dt} + B_{m,red} \omega_m + T_{dist} \quad (11)$$

Where  $J$  is the total system inertia and  $T_{dist}$ , the disturbance torque, consists of the load torque and Coulomb friction. The total system inertia includes the inertia of both the IM and PMSM machine and also the coupling and fastening components between them.

The first term is related to the torque needed to accelerate the system without friction, the last two terms are related to the torque which is needed to overcome the viscous friction and the disturbance torque, respectively. Disturbance torque may be load torque, non-modelled friction (etc.) in the given system.

### 3 DESIGN OF CONTROLLERS

In this chapter, the control scheme of the SPMSM motor is explained shortly, namely the Field Oriented Control (FOC). This chapter is heavily based on [1].

#### 3.1 Field Oriented Control

Field Oriented Control (FOC) is a widely used control technique for controlling AC machines due to its efficiency. The idea of FOC is to control the torque and the flux-linkage separately. For an SPMSM when the current vector is chosen to be on the *q*-axis, this results in a maximum-torque-per-ampere (MTPA) operation.

#### 3.2 Control Design

The main objective of the controller is to regulate the speed of the machine. To achieve this, a cascade control structure is implemented, where the outer loop is a speed controller and the inner loop consists of two current controllers. The two current controllers control the *d*-axis current and *q*-axis current. The reference *q*-axis current is calculated by the speed controller from the determined necessary torque to keep tracking the speed reference. For this control structure, the bandwidth of the outer loop should be 5 ~ 10 times lower than the inner loop to avoid interference between the controllers. Using this knowledge, the inner loop can be reduced to a first-order system.

The control loops are designed as a continuous transfer function and then discretized transfer functions are found with similar characteristics. This is achieved by taking into consideration the delays present in the system and the sampling frequency of the system. This is called design-by-emulation.

The criteria for the control system is presented here in table 2. It is not listed in the table, but of course, it is paramount that the system is stable.

Table 2: Design Criteria of control loops

	Max. Overshoot	Bandwidth	Steady-State Error
Current Loop	5%	High as possible	Zero
Speed Loop	15%	High as possible	Zero

Figure 2 shows the full structure of the field-oriented control.

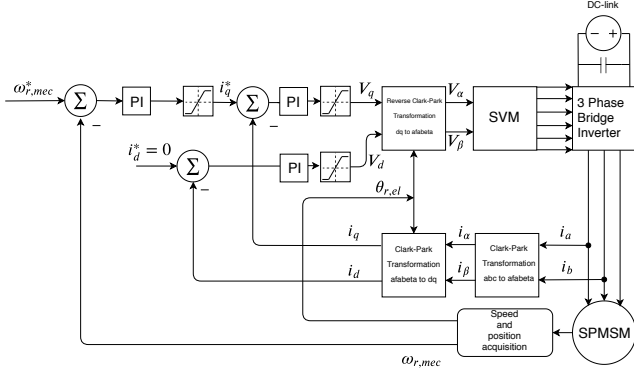


Figure 2: Field Oriented Control scheme.

### 3.3 Design of Current Controllers

The following section discusses the design process of the current control loops used in FOC [1].

The current controllers are the inner loop controlling the stator currents. To fulfill the design criteria, the system type is increased to 1 which results in no steady-state error for a step input.

After decoupling the system, the transfer function for both q-axis and d-axis are derived as shown in equation (12) and equation (13)

$$G_d = \frac{i_d}{v_d} = \frac{1}{sL_d + R_s} \quad (12)$$

$$G_q = \frac{i_q}{v_q} = \frac{1}{sL_q + R_s} \quad (13)$$

The resulting open-loop transfer function, including the controller and the delays, is shown in equation (14).

$$G_{ol}(s) = \frac{K_i + sK_p}{s} \frac{1}{st_d + 1} \frac{1}{sL_d + R_s} \quad (14)$$

The design of the control parameters was done using pole placement and SISOTOOL in Matlab with the design criteria as guidance. Because for an SPMSM,  $d$ - and  $q$ -axis inductance are the same ( $L_d = L_q$ ), the controllers can be designed using only the  $d$ -axis. Analyzing the transfer functions, it is apparent that there is a dominant pole. The dominant pole in the system is canceled by designing the PI zero accordingly.

### 3.4 Design of Speed Controllers

The following section explains the design process of the speed control loop for the FOC [1]. A PI controller is a good choice here too because it can effectively compensate for the disturbances torque present in the system. The controller also improves the transient response of the system. It is expected that the speed loop, is much slower than the current loops. Due to this, the current loops will be reduced to a first-order system that has the same settling time as the actual current loops.

First, the inner loop is reduced to the first-order system from the third order. The new time constant is acquired by:  $\tau = t_{settling}/4$ . The transfer function then becomes equation (15).

$$G_{IL} = \frac{1}{\tau s + 1} \quad (15)$$

The next step is to derive the transfer function for the mechanical system. The mechanical equation from Newton's second law is repeated in equation (16).

$$T_e = J \frac{d\omega_m}{dt} + B_m \omega_m + T_{dist} \quad (16)$$

Equation (16) is transformed into the Laplace domain where the disturbances are put to be zero, to ensure that controllers are designed the overshoot is the highest. The transfer function representing the mechanical system is formed by combining (10) and (16) resulting in the following equation:

$$\frac{\omega_m}{i_q} = \frac{K_{C2T}}{Js + B_m} \quad (17)$$

Where  $K_{C2T} = \frac{3}{2} N_{pp} \lambda_{mpm}$ . The block diagram of the speed loop is shown in figure 3.

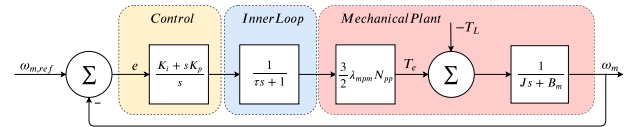


Figure 3: Block diagram of the speed loop.

The control parameters for the speed loop controller were designed similarly as the current loop controller, namely with pole placement and SISOTOOL. In figure 4 the open loop transfer function of the speed loop is shown where the phase margin of the system is 85.8degree. This means that the system is stable. In this diagram the gain is  $K_p = 1$ , and oscillation is not expected in a step response.

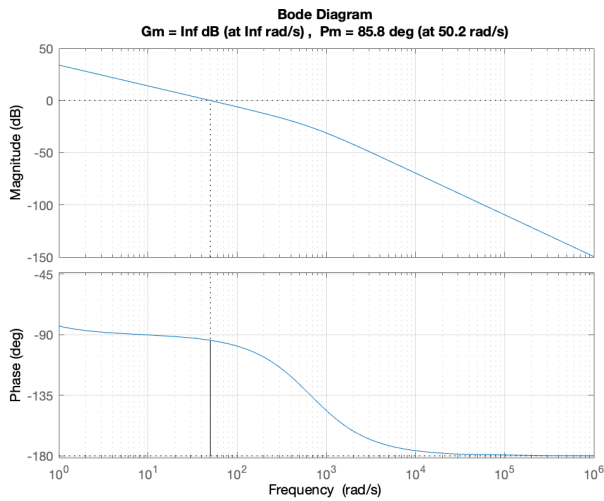


Figure 4: Bode Diagram showing open loop transfer function of the speed loop.

In figure 5 the bode diagram of the closed-loop transfer function of the speed and current loop is shown.

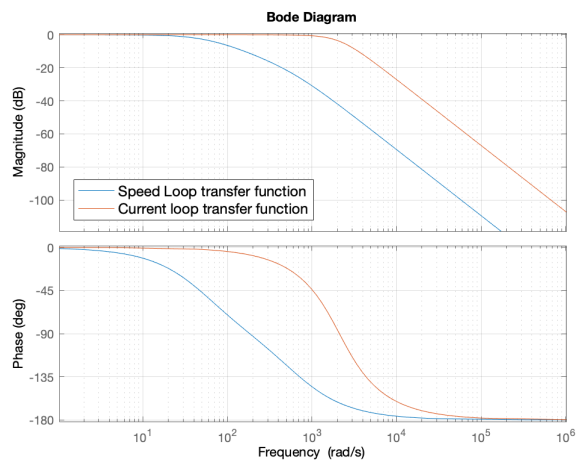


Figure 5: Bode Diagram showing closed loop transfer function of the speed and current loop.

From the figure, it is clear that the inner loop is faster than the outer. The bandwidth of the inner loop is  $2400 \text{ rad/s}$  and the bandwidth of the outer loop is  $54 \text{ rad/s}$  which means that the requirement for cascade control, is fulfilled.

## 4 CONCLUSION

Everything works as expected.

## REFERENCES

- [1] B. Temesi, U. G. Gautadottir, *Sensorless Control of PMSM Drive Using Sliding-Mode-Observers* AAU, Denmark, 2020 Master's thesis.
- [2] D. Wilson, *Motor Control Compendium*, 1st-ed . 2011

- [3] K. Lu, *Control of Electrical Drive Systems and Converts Lecture 1 Slides*, 1st-ed . pp. 1-30, 2019
- [4] C. L. Philips, R. D. Harbor, *Feedback Control Systems*, 1st-ed . 4th Editio. New Jersey: Prentice Hall, 2000, isbn: 0-13-949090-6.